ANALYZING THE CHEMICAL AND SPECTRAL EFFECTS OF PULSED LASER IRRADIATION TO SIMULATE SPACE WEATHERING OF A CARBONACEOUS CHONDRITE. M. S. Thompson[1], L. P. Keller[1], R. Christoffersen[2], M. J. Loeffler[3], R. V. Morris[1], T. G. Graff[2], and Z. Rahman[2], [1]ARES, NASA/JSC, Houston, TX 77058, [2]Jacobs, NASA Johnson Space Center, Mail Code XI3, Houston, TX, [3]NASA GSFC, Greenbelt, MD 20771, USA, michelle.s.thompson@nasa.gov.

Introduction: Space weathering processes alter the chemical composition, microstructure, and spectral characteristics of material on the surfaces of airless bodies. The mechanisms driving space weathering include solar wind irradiation and the melting, vaporization and recondensation effects associated with micrometeorite impacts e.g., [1]. While much work has been done to understand space weathering of lunar and ordinary chondritic materials, the effects of these processes on hydrated carbonaceous chondrites is poorly understood. Analysis of space weathering of carbonaceous materials will be critical for understanding the nature of samples returned by upcoming missions targeting primitive, organic-rich bodies (e.g., OSIRIS-REx and Hayabusa 2).

Recent experiments have shown the spectral properties of carbonaceous materials and associated minerals are altered by simulated weathering events e.g., [2-5]. However, the resulting type of alteration i.e., reddening vs. bluing of the reflectance spectrum, is not consistent across all experiments [2-5]. In addition, the microstructural and crystal chemical effects of many of these experiments have not been well characterized, making it difficult to attribute spectral changes to specific mineralogical or chemical changes in the samples. Here we report results of a pulsed laser irradiation experiment on a chip of the Murchison CM2 carbonaceous chondrite to simulate micrometeorite impact processing.

Samples and Methods: We performed pulsed laser experiments by scanning a Nd-YAG laser at its fundamental wavelength (1064 nm) (pulse width ~6 ns) once over the sample. The average laser energy per pulse was 48 mJ, similar to [2]. A glass slide was placed above the sample enabling the collection of the recondensed vapor plume produced by the irradiation, similar to [6]. We obtained reflectance spectra from both the unirradiated and irradiated samples, as well of the vapor deposit using an ASD FieldSpec 3 Spectrometer (0.35–2.5 μm). The spectra were measured relative to a LabSphere Spectralon standard using the ASD contact probe. A JEOL 7600F field emission scanning electron microscope (SEM) with x-ray detector system was used to study the morphological and chemical effects of irradiation on the meteorite chip. An electron transparent thin section was prepared from the vapor deposit using the FEI Quanta 3D focused ion beam (FIB) instrument. The section was analyzed using the JEOL 2500SE scanning transmission electron microscope (STEM) equipped with a Thermo thin window energy-dispersive X-ray (EDX) spectrometer. Quantitative spectrum imaging was completed using a 2 nm probe.

Results from Spectral Analysis: The reflectance spectrum collected from the irradiated Murchison chip is darker than the unirradiated sample. The spectrum collected from the vapor deposit is strongly reddened in the visible and near-IR wavelengths (Fig. 1).

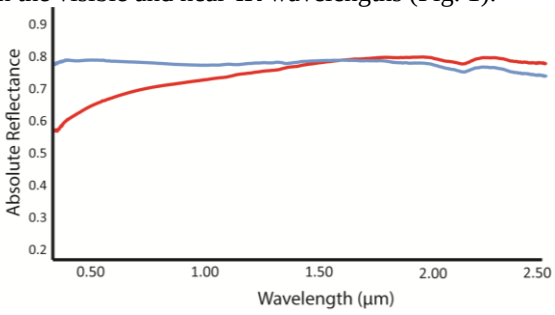

Figure 1: Reflectance spectra collected for the plain glass slide (blue) and the slide containing the vapor deposit, (red), both backed by the Spectralon standard. Note strong reddening across the visible wavelengths in the vapor deposit.

Microchemical and Structural Analysis: SEM analysis of the meteorite matrix show textures consistent with melting and possible outgassing of volatile species (e.g., burst vesicles) as a result of laser irradiation (Fig. 2). Mineral grains exhibit a varied response to irradiation. Iron sulfide grains also show the development of a vesiculated/melted surface in response to laser irradiation (Fig. 2). Olivine grains in chondrules and as isolated grains in the matrix display localized regions of melting, but otherwise show very little change in surface morphology (Fig. 2).

TEM analysis of the thin section extracted from the vapor deposit reveals the presence of a chemically and structurally complex deposit of non-uniform thickness. Ranging between 30 - 350 nm in thickness, the deposit exhibits a stratified chemical composition indicative of multiple, distinct emplacement events (Fig. 3). Distributed nearly uniformly across the section is a thin (~50 nm) deposit, typically rich in Fe and S, which may represent recondensation of an initial vapor cloud. Overlying this vapor deposit in several locations are thicker (up to ~250 nm) layers enriched in Mg, Si, Fe, and occasionally Ca. These layers have a unique morphology, forming pancake-like shapes with uniform

thicknesses and rounded ends. The morphology, thickness, and more refractory composition of these layers compared to the vapor deposits, indicates they are likely melt deposits, emplaced when a spherical melt droplet generated during the irradiation event impacted the suspended glass slide before final solidification. Superimposed on many of these melt features is another thin (30 - 50 nm) layer enriched in volatile species, e.g., Fe and S, which may represent a second vapor deposit (Fig. 3). While this exterior layer may have been emplaced during the same event responsible for producing the initial vapor and melt deposits, this layer could also be sourced from a second, later laser pulse which targeted an adjacent area of the sample. Each of these stratigraphic layers exhibit vesiculated textures, likely formed via outgassing of volatile species during cooling.

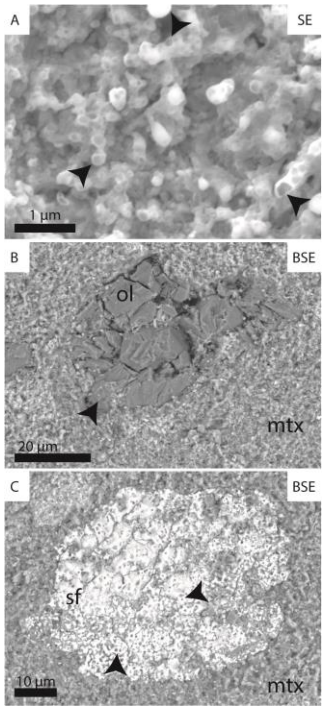

Figure 2: A) Secondary electron image showing the melted texture of the surface of the irradiated Murchison matrix. Hollow, burst vesicles are indicated by black arrowheads. B) Backscattered electron image of olivine grains surrounded by matrix material. Localized melting indicated by the black arrowhead. C) Backscattered electron image of a sulfide grain. Black arrowheads indicate pits on the surface of the material which formed by laser irradiation.

In addition to vesicles, there are nanoparticles present throughout both the melt and vapor deposits. Nanoparticles in the vapor layers are typically smaller in size (as small as 2-3 nm) whereas those found in the melt layers are larger (up to 20 nm in diameter), similar to results reported for lunar samples [7]. The mineralogy of the nanoparticles is variable. Selected area electron diffraction patterns collected for nanoparticle-bearing deposits indicate at least three phases are present: troilite (FeS), pentlandite ($(FeNi)_9S_8$), and magnetite (Fe_3O_4). These structural phase identifications are supported by the extraction of EDS spectra from isolated nanoparticles which yield compositions consistent with Fe and Ni bearing sulfides and Fe-oxides.

Implications for Space Weathering on Primitive Bodies: The results presented here indicate that space weathering processes affect carbonaceous materials in similar ways when compared to their lunar and ordinary-chondritic counterparts. Micrometeorite impact events (simulated with laser irradiation) produce textures consistent with melting of the substrate, and generate a vapor plume which subsequently recondenses with a distinctive chemical composition. The high water and volatile content of carbonaceous materials produce vesiculated textures, both in the matrix of the substrate and in the recondensed phases. The presence of small nanoparticles in the vapor condensate is likely responsible for the reddening we observe across the visible wavelengths of the associated reflectance spectrum. The identification of nanophase Fe-sulfides is consistent with previous experiments suggesting the importance of these phases in asteroidal space weathering [6]. Finally, the presence of water in the meteorite, and consequently in the vapor plume, may play an important oxidizing role in the condensation of nanoparticles. While nanoparticles in lunar soils typically condense in the Fe^0 phase, here we see a significant contribution from oxidized Fe in the nanophase. Magnetite grains have been shown to redden reflectance spectra less efficiently than Fe^0 [8]. As such, the production of Fe-oxide nanoparticles may contribute to the inconsistency in reddening/bluing of spectra collected from materials that have experienced simulated weathering processes.

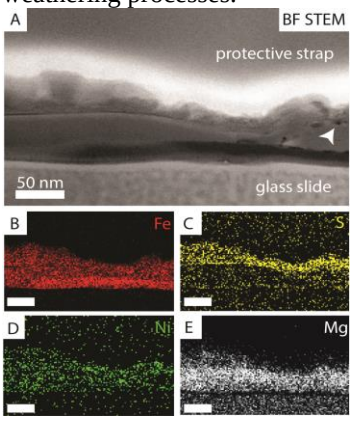

Figure 3: A) BF STEM image showing the complex stratigraphy of the melt and vapor deposit. The white arrow indicates the location of a nanophase Fe-Ni-S grain. EDS maps of the region showing the distribution of B) Fe, C) S, D) Ni, and E) Mg. Scale bars are all 50 nm.

References: [1] Pieters C. M. and Noble S. K. (2016) *J. Geophys. Res-Planet., 121*, 1865-1884. [2] Kaluna H. M. et al. (2017) *Icarus,* http://dx/doi.org/10.1016/j.icarus.2016.12.028. [3] Matsuoka M. et al. (2015) *Icarus, 254*, 135-143. [4] Gillis-Davis J. J. et al. (2015) *LPSC XXXXVI*, Abstract 1607. [5] Moroz L. et al. (2004) *Icarus, 170*, 214-228. [6] Keller L. P. et al. (2013) *LPSC XXXXIV*, Abstract 2404. [7] Keller L. P and Clemett S. J. (2001) *LPSC XXXII*, Abstract 2097. [8] Thompson M. S. et al. (2016) *Meteorit. Planet. Sci., 51*, 1082-1095.